ISBN: 978-3-95450-232-5 ISSN: 2673-7000 doi:10.18429/JACoW-NAPAC2022-TUPA16

# SINGULARITY-FREE EXACT DIPOLE BEND TRANSPORT EQUATIONS

David Sagan*, Cornell University, Ithaca, NY, USA

*Abstract*

Exact transport equations for a pure dipole bend (a bend with a dipole field and nothing else) have been derived and formulated to avoid singularities when evaluated. The transport equations include finite edge angles and no assumption is made in terms of the bending field being matched to the curvature of the coordinate system.

## INTRODUCTION

Pure dipole bend elements, that is bends with a pure dipole field and no higher order multipoles, are ubiquitous in lattices used to simulate many machines such as the LHC, SuperKEKB, RHIC, BEPC, etc., etc. Despite the fact that such a bend is conceptionally simple (the particle motion is circular), there is a wide range of algorithms used for particle tracking. For example, the MAD8 program uses a second order map [1], SixTrack uses splitting to approximately solve the exact Hamiltonian [2], PLACET [3] uses a linear matrix in the transverse coordinates with the bending strength scaled by the particle energy, the SAD program [4] implements an exact solution [4], and Elegant implements several tracking methods depending upon which type of bend is chosen [5].

An exact tracking solution [4, 6, 7] is to be preferred over an approximate one. However, up to now, the published algorithms for the exact solution suffer from singularities in the limit of zero reference bending angle or zero field. The singularities are removable, however, since the formulas involve multiple variables, this complicates implementation. To simplify matters, this paper formulates the exact solution in such a way as to avoid any singularities except for the standard $\mathrm{sinc}(x) = \sin(x)/x$ function which is easily coded to be well behaved even in the vicinity of zero. The transport equations include finite edge angles and no assumption is made in terms of the bending field being matched to the curvature of the coordinate system.

Not covered here is tracking through fringe fields so the tracking algorithm assumes a hard edge to the dipole field. The algorithm is divided into three parts: entrance tracking for a finite entrance face angle $e_1$, tracking the sector body, and finally tracking for a finite exit face angle $e_2$.

## SECTOR BODY TRACKING

This section covers tracking through the body of the dipole which is taken to be a sector bend as illustrated in Fig. 1. The particle phase space coordinate system used for the analysis is $(x, p_x, y, p_y, z, p_z)$ where

$$p_{x,y} = \frac{P_{x,y}}{P_0}, \quad z = -\beta c(t - t_0), \quad p_z = \frac{P - P_0}{P_0} \tag{1}$$

* Work supported in part by Department of Energy grant DE-SC0018370.

with $P_{x,y}$ being the transverse momentum, $P$ is the momentum, $P_0$ is the reference momentum, $\beta c$ the particle velocity, $t$ the time, and $t_0$ the reference time.

The particle's phase space coordinates are expressed with respect to a geometric $(x, y, x)$ curvilinear coordinate system. The $(x, y, s)$ coordinate system at the entrance to the dipole has origin at $O_1$ with $y$ perpendicular to the plane of the dipole, and $x$ and $s$ in the plane of the dipole with $x$ along the entrance edge, and $s$ perpendicular to the entrance edge. The $(x, y, s)$ coordinate system at the exit end has the origin at $O_2$ and has a similar orientation with respect to the exit edge as the entrance coordinates with respect the entrance edge.

As shown in Figure 1, at point 1 where the particle enters the bend, $\phi_1$ is the angle of the particle trajectory in the plane of the bend with respect to the $s$ axis. In terms of the entrance phase space coordinates, $\phi_1$ is

$$\sin(\phi_1) = \frac{p_{x1}}{\sqrt{(1 + p_z)^2 - p_y^2}} \tag{2}$$

where the subscript "1" for $p_z$ and $p_y$ is dropped since these quantities are invariant.

The $(u, v)$ coordinate system in the plane of the bend is defined with the $u$-axis along the exit edge of the bend and the $v$-axis is perpendicular to the $u$-axis. The origin is at the design center of the bend. The point $(u_1, v_1)$ where the particle enters the bend is given by

$$u_1 = (\rho + x_1)\,\cos(\theta) \tag{3}$$

$$v_1 = (\rho + x_1)\,\sin(\theta) \tag{4}$$

where $\rho$ is the design radius of curvature, $x_1$ is the offset of the particle from the design at the entrance point, and $\theta$ is the design bend angle

$$\theta = \frac{L}{\rho} = g\,L \tag{5}$$

with $L$ being the design arc length and $g \equiv 1/\rho$.

The coordinates $(u_0, v_0)$ of the center of curvature of the particle trajectory is

$$u_0 = u_1 - \rho_p\,\cos(\theta + \phi_1) \tag{6}$$

$$v_0 = v_1 - \rho_p\,\sin(\theta + \phi_1) \tag{7}$$

where $\rho_p$ is the radius of curvature of the particle trajectory in the $(u, v)$ plane

$$g_p = \frac{1}{\rho_p} = \frac{g_{\mathrm{tot}}}{\sqrt{(1 + p_z)^2 - p_y^2}} \tag{8}$$

with $g_{\mathrm{tot}}$ being the bending strength of the actual field as opposed to $g$ which is the bending strength defined by the geometry of the sector.

ISBN: 978-3-95450-232-5 ISSN: 2673-7000 doi:10.18429/JACoW-NAPAC2022-TUPA16



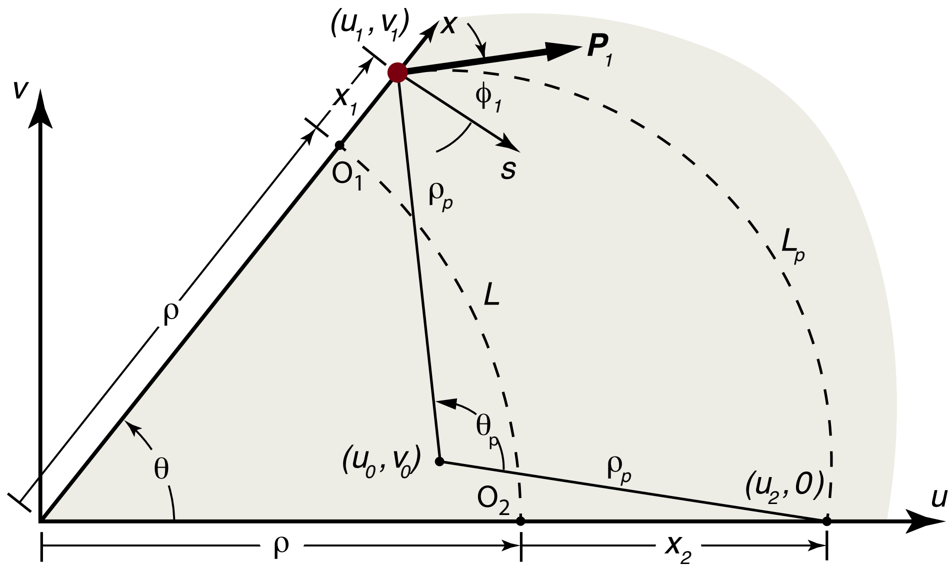


Figure 1: Geometry for the exact bend calculation. The particle starts at $(u_1, v_1)$ on the entrance edge and travels to point $(u_2, 0)$ on the exit edge.

The coordinates of the particle at the exit face is $(u_2, 0)$ where

$$u_2 = u_0 + \sqrt{\rho_p^2 - v_0^2} \tag{9}$$

After some manipulation, the offset of the particle $x_2$ from the design point at the exit face is

$$x_2 = u_2 - \rho = x_1 \cos(\theta) - \frac{g}{2} L^2 \operatorname{sinc}^2(\theta/2) + \xi \tag{10}$$

where, as discussed in the introduction, $\operatorname{sinc}(x)$ is the standard $\sin(x)/x$ function. $\xi$ in the above equation can be expressed in two different ways

$$\xi = \frac{\alpha}{\left[\cos^2(\theta + \phi_1) + g_p\,\alpha\right]^{1/2} + \cos(\theta + \phi_1)} \tag{11}$$

or

$$\xi = \frac{\left[\cos^2(\theta + \phi_1) + g_p\,\alpha\right]^{1/2} - \cos(\theta + \phi_1)}{g_p} \tag{12}$$

where

$$\alpha = 2\,(1 + g\,x_1)\,\sin(\theta + \phi_1)\,L \operatorname{sinc}(\theta) - g_p\,(1 + g\,x_1)^2\,L^2 \operatorname{sinc}^2(\theta) \tag{13}$$

Both Eq. (11) and Eq. (12) are needed since Eq. (11) is singular when $\alpha = 0$ and $\theta + \phi_1 = \pi$ (which happens when the particle is bent by 180°), and Eq. (12) is singular when $g_p$ is zero. A simple way to implement the calculation to avoid these singularities is to use Eq. (11) when $|\theta + \phi_1| < \pi/2$ and otherwise use Eq. (12).

Once $x_2$ is computed, the arc length of the particle $L_p$ is

$$L_p = \frac{|\mathbf{L}_c|}{\operatorname{sinc}(\theta_p/2)} \tag{14}$$

where $\mathbf{L}_c$ is the vector (chord) from point 1 and point 2

$$\mathbf{L}_c = (L_{cu}, L_{cv}) = (\xi, -L \operatorname{sinc}(\theta) - x_1 \sin(\theta)) \tag{15}$$

and $\theta_p$ is the angle made by the particle trajectory which is twice the angle between the initial particle trajectory $\mathbf{P}$ and the vector $\mathbf{L}_c$

$$\theta_p = 2\,(\theta + \phi_1 - \operatorname{atan2}(L_{cu}, -L_{cv})) \tag{16}$$

where $\operatorname{atan2}(y, x)$ is the standard two argument arctangent function.

Once $L_p$ is computed, $p_{x2}$, $y_2$ and $z_2$ phase space coordinates at the exit edge are easily calculated

$$p_{x2} = \sqrt{(1 + p_z)^2 - p_y^2}\,\sin(\theta + \phi_1 - \theta_p) \tag{17}$$

$$y_2 = y_1 + \frac{p_y\,L_p}{\sqrt{(1 + p_z)^2 - p_y^2}} \tag{18}$$

$$z_2 = z_1 + \frac{\beta\,L}{\beta_{\text{ref}}} - \frac{(1 + p_z)\,L_p}{\sqrt{(1 + p_z)^2 - p_y^2}} \tag{19}$$

where $\beta$ is the normalized velocity of the particle and $\beta_{\text{ref}}$ is the normalized velocity of the reference particle.

## EDGE TRACKING

For bends where the pole faces are rotated with respect to the nominal sector geometry, the above algorithm must be extended. The geometry for the entrance face is shown in Figure 2. The angle $e_1$ is the rotation of the edge of the bend (where the field starts) about the origin point $O_1$. It is assumed that the propagation of the particle in the lattice element previous to the bend will always leave the particle at the sector edge (green dot in the figure) independent of $e_1$. To account for a finite $e_1$ the following steps need to be taken:

ISBN: 978-3-95450-232-5 ISSN: 2673-7000 doi:10.18429/JACoW-NAPAC2022-TUPA16

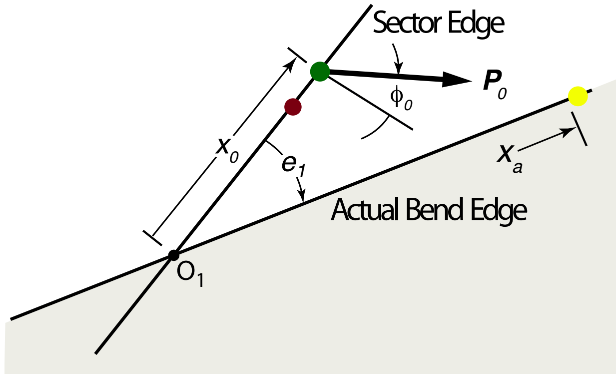


Figure 2: Entrance face geometry with a finite $e_1$ face angle. The actual bend edge where the field starts is rotated from the "sector edge". A similar situation occurs at the exit edge. The particle starts (green dot) at a distance $x_0$ from the origin $O_1$ of the edge rotation. The particle is drifted to the actual bend edge (yellow dot) and then propagated as if in the dipole field back to the sector edge (red dot).

1. Drift (propagate in a straight line) the particle from the sector edge to the actual bend edge (yellow dot). The propagation may be forward or backwards depending upon on the signs of $x_0$, the distance from $O_1$ to the particle, and $e_1$.

   The particle drifts a distance $L_a$ to the actual bend edge at a distance $x_a$ from $O_1$. $L_a$ and $x_a$ are computed via

$$\begin{aligned} L_a &= \frac{x_0 \sin(e_1)}{\cos(e_1 + \phi_0)} \\ x_a &= \frac{x_0 + L_a \sin(\phi_0)}{\cos(e_1)} \end{aligned} \tag{20}$$

   where $\phi_0$ is the angle of the particle trajectory with respect to the perpendicular of the sector edge.

2. Propagate the particle as if it were in the dipole field from the actual bend edge to the sector edge (red dot). Again the propagation may be forward or backwards depending upon on the signs of $x_0$ and $e_1$.

   The same equations as in the previous section can be used with the substitution

$$\begin{aligned} \theta &\to -e_1 \\ 1 + g\, x_1 &\to x_0 \end{aligned} \tag{21}$$

The particle can now be propagated throughout the body of the bend as discussed in the previous section.

At the exit end, with pole face rotation $e_2$, the process is reversed

1. Propagate the particle as if in the dipole field from the exit sector edge to the exit actual bend edge.

2. Drift the particle from the actual exit bend edge to the exit sector edge.

## CONCLUSION

The exact solution to tracking through a pure dipole field has been presented in such a way as to avoid singularities in the equations. The algorithm includes the handling of finite face angles at the entrance and/or exit ends. Not covered are fringe fields. The exact bend equations have been implemented in the PTC library [8] and the Bmad software toolkit [9] for charged-particle simulations.

## ACKNOWLEDGMENTS

Thanks to Étienne Forest for useful discussions and for all the help he has given over the years to explaining things and for his help in integrating PTC with Bmad.

## REFERENCES

[1] F. C. Iselin, "The MAD Program, Physical Methods Manual," CERN, Tech. Rep. CERN/SL/92-?? (AP), 1994. https://mad8.web.cern.ch/mad8/doc/phys_guide.pdf

[2] M. Fjellstrom, "Particle Tracking in Circular Accelerators Using the Exact Hamiltonian in SixTrack," M.S. thesis, Lulea U., 2013. https://inspirehep.net/literature/1339695

[3] J. Snuverink and J. Pfingstner, "Linear accelerator simulation framework with placet and guinea-pig," Tech. Rep. CLIC-Note-1064, 2015. http://cds.cern.ch/record/2145365

[4] D. Zhou and K. Oide, "Maps used in sad (draft)," 2014.

[5] M. Borland, *User's manual for elegant*, 2022.0, Argonne National Laboratory, 2022.

[6] E. Forest, *Beam Dynamics, A New Attitude and Framework*. Taylor & Francis, 1998. https://books.google.com/books?id=5p4gka0a2ScC

[7] A. Sharma, P. Singh, Abdurrahim, A. D. Ghodke, and G. Singh, "Analytical expressions of transfer functions for a hard edge dipole magnet using a basic geometrical approach," *Phys. Rev. ST Accel. Beams*, vol. 16, no. 1, p. 014 001, 2013. doi:10.1103/PhysRevSTAB.16.014001

[8] F. Schmidt, E. Forest, and E. McIntosh, "Introduction to the polymorphic tracking code: Fibre bundles, polymorphic Taylor types and "Exact tracking"," CERN, Tech. Rep. CERN-SL-2002-044-AP, KEK-REPORT-2002-3, 2002. http://cds.cern.ch/record/573082

[9] D. Sagan, "Bmad: A relativistic charged particle simulation library," *Nucl. Instrum. Methods Phys. Res., Sect. A*, vol. 558, no. 1, pp. 356–359, 2006. doi:10.1016/j.nima.2005.11.001